

Temperature-Induced Aggregation of Poly(*N*-isopropylacrylamide)-Stabilized CdS Quantum Dots in Water

Jing Ye,[†] Yi Hou,[‡] Guangzhao Zhang,^{*,†,‡,§} and Chi Wu^{†,‡,§}

Department of Chemistry, The Chinese University of Hong Kong, Shatin, N.T., Hong Kong, China, Department of Chemical Physics, University of Science and Technology of China, and The Hefei National Laboratory for Physical Sciences at Micro-scale, Hefei, Anhui 230026, China

Received October 1, 2007. In Final Form: November 27, 2007

Water-soluble nanosized semiconductor CdS particles (quantum dots, QDs) were synthesized with a protective layer of covalently grafting linear thermally sensitive poly(*N*-isopropylacrylamide) chains. Reversible association and dissociation of these CdS particles can be induced via an alteration of the solution temperature. The formation and fragmentation of the QD aggregates of the CdS particles were systematically investigated by laser light scattering (LLS) and confirmed by transmission electron microscopy (TEM). There exists a hysteresis during one heating-and-cooling cycle. The CdS particles stabilized with shorter PNIPAM chains ($M_n = 15\,000$ g/mol) can associate to form larger and denser spherical aggregates with a much higher aggregation number than those grafted with longer PNIPAM chains ($M_n = 31\,000$ g/mol) in the heating process. The dissociation (fragmentation) in the cooling process has two stages: initially, the aggregates dissociate as the temperature decreases, and then, the fragmentation stopped over a wider temperature range before complete dissociation. We attribute such a two-stage fragmentation to a balanced effect of inter- and intrachain hydrogen bonding as well as the hydrophobic interaction between PNIPAM chains and CdS particles.

Introduction

Nanometer-sized semiconductor particles, or quantum dots (QDs), have been extensively studied and still remain an active research area because of their unique size- and surface-dependent nonlinear optical, physicochemical, and electronic properties.^{1–3} Various methods for the preparation of high-quality QDs, specifically CdSe, CdTe, CdS, and ZnS, have been developed.^{4–6} For example, in a traditional synthetic route, CdSe nanocrystals can be synthesized by the pyrolysis of dimethyl cadmium ($\text{Cd}(\text{CH}_3)_2$) within tri-*n*-octylphosphine (TOP) and tri-*n*-octylphosphine oxide (TOPO).² However, the pyrolysis of toxic organometallic reagents in an organic solvent is not environmentally friendly. For biomedical and environmental applications, desirable water-soluble QDs can be produced by further functionalizing the surface of QDs with thiol or amine groups. On this approach, various low molar mass thiol-functional molecules have been used as stabilizers in the preparation of stable colloid dispersions of QDs.^{7–10} On the other hand, long polymer chains with a functional group are also used as stabilizers for the preparation of water-soluble QDs. Using long polymer chains has some additional advantage over low molar mass ligands. For example,

they can be used to prepare a thin film with a controllable interparticle distance. Carrot et al.¹¹ had successfully synthesized nanosized CdS particles stabilized by long polyester chains with a thiol end group. During the reaction, there is a competition between the growth of CdS crystals and the surface capping by linear thiol-bearing polymer chains that results in small particles with a CdS core and a covalently bonded protective polymer shell.

Furthermore, it has recently been recognized that the utilization of QDs as a building block for some useful devices requires a better understanding of how to make them self-organize into some controllable superstructures on different functional length scales. For example, the incorporation of QDs into a polymeric material offers the added advantage of combining the unique properties of QDs with some specified mechanical, optical, and electronic properties of polymers. To make a QDs/polymer composite, the association and dissociation of QDs play an essential role in their eventual properties. Eisenberg et al.¹² studied the association of CdS stabilized by polystyrene-*b*-poly(acrylic acid) copolymer chains in aqueous solutions with varying polymer/CdS ratios. However, the resultant aggregates are large, polydispersed, and sometimes precipitated out of the dispersions. It still remains a challenge to produce monodispersed and size-adjustable CdS QDs in aqueous solutions.

Hybrid core-shell particles with an inorganic core and a chemically bonded polymer brush layer (shell) should be better than QDs stabilized by the adsorption of a layer of copolymer chains. This is why different strategies have been used to generate polymer stabilized QDs, in which “grafting-from” and “grafting-to” approaches have been applied. Using environmentally sensitive polymers^{13,14} can offer an additional advantage, because self-association/dissociation of these QDs can be triggered by an

* Corresponding author. The Hefei address should be used for all correspondence. E-mail: gzzhang@ustc.edu.cn.

[†] The Chinese University of Hong Kong.

[‡] University of Science and Technology of China.

[§] The Hefei National Laboratory for Physical Sciences at Micro-scale.

(1) Chen, Y.; Rosenzweig, Z. *Nano Lett.* **2002**, *2*, 1299.

(2) Murray, C. B.; Norris, D. J.; Bawendi, M. G. *J. Am. Chem. Soc.* **1993**, *115*, 8706.

(3) Farmer, S. C.; Patten, T. E. *Chem. Mater.* **2001**, *13*, 3920.

(4) Spanhel, L.; Haase, M.; Weller, H.; Henglein, A. *J. Am. Chem. Soc.* **1987**, *109*, 5649.

(5) Tomasulo, M.; Yildiz, I.; Raymo, F. M. *J. Phys. Chem. B.* **2006**, *110*, 3853.

(6) Foglia, S.; Suber, L.; Righini, M. *Colloids Surf.* **2001**, *177*, 3.

(7) Vossmeier, T.; Katsikas, L.; Giersig, M.; Popovic, I. G.; Diesner, K.; Chemseddine, A.; Eychmuller, A.; Weller, H. *J. Phys. Chem.* **1994**, *98*, 7665.

(8) Kho, R.; Torres-Martinez, C. L.; Mehra, R. K. *J. Colloid Interface Sci.* **2000**, *227*, 561.

(9) Sapra, S.; Nanda, J.; Sarma, D. D.; El-Al, F.; Hodes, G. *Chem. Commun.* **2001**, 2188

(10) Chen, Y. F.; Rosenzweig, Z. *Anal. Chem.* **2002**, *74*, 5132.

(11) Carrot, G.; Scholz, S. M.; Plummer, C. J. G.; Hilborn, J. G. *Chem. Mater.* **1999**, *11*, 3571.

(12) Moffitt, M.; Vali, H.; Eisenberg, A. *Chem. Mater.* **1998**, *10*, 1021.

(13) Raula, J.; Shan, J.; Nuopponen, M.; Niskanen, A.; Jiang, H.; Kauppinen, E. I.; Tenhu, H. *Langmuir* **2003**, *19*, 3499.

(14) Shan, J.; Chen, J.; Nuopponen, M.; Tenhu, H. *Langmuir* **2004**, *20*, 4671.

external stimulations, such as alteration of pH, ionic strength, and temperature.

Poly(*N*-isopropylacrylamide) (PNIPAM), as a well-known and well-studied water-soluble thermally sensitive polymer, has an easily accessible lower critical solution temperature (LCST ~ 32 °C).^{15,16} Namely, PNIPAM is hydrophilic and soluble in water as individual random-coil chains when the temperature is lower than LCST. As the solution temperature increases, PNIPAM becomes hydrophobic and insoluble in water to form single-chain globules or multichain aggregates (mesoglobules).^{17–19} Such a reversible conformational change with the solution temperature has made PNIPAM and its derivatives useful in a wide range of biorelated applications. In the current study, we have used a direct and simple synthetic method to produce core–shell CdS QDs with a CdS core and a layer of covalently grafted linear PNIPAM chains (shell) at the room temperature. Two different PNIPAM chains (31 000 and 15 000 g/mol) were used. The association and dissociation of these PNIPAM-grafted CdS QDs in aqueous solutions was systematically studied by using laser light scattering (LLS) and transmission electron microscopy (TEM).

Experimental Section

Sample Preparations. CdS quantum dots were prepared by injecting an appropriate amount of sodium sulfide into cadmium acetate aqueous solution at 40 °C with vigorous stirring. The filtration with a 0.8 μm Millipore filter led to the final product. The average diameter of the QDs was estimated to be ~ 5 nm by TEM. The dithioester-terminated PNIPAM chains with two different lengths were synthesized by reversible addition–fragmentation chain transfer polymerization in tetrahydrofuran (THF),²⁰ in which cyanoisopropyl dithiobenzoate and 4,4'-azobis(isobutyronitrile) were used as the chain transfer agent and initiator. The molar mass (M_n) and polydispersity index (M_w/M_n) of the PNIPAM chains were measured by size exclusion chromatography (SEC) on Waters 1515 by using monodisperse polystyrene as standard and THF as eluent with a flow rate of 1.0 mL/min at 35 °C. For the short PNIPAM chains, $M_n = 15$ 000 g/mol and $M_w/M_n = 1.16$. For the longer PNIPAM chains, $M_n = 31$ 000 g/mol and $M_w/M_n = 1.09$. Thiolated PNIPAM chains (PNIPAM–SH) were subsequently prepared by the reduction of dithioester-terminated ends with NaBH_4 . Finally, a solution of CdS QDs in water was added dropwise into PNIPAM–SH aqueous solution under magnetic stirring and the mixture was further stirred for 3 days at room temperature, yielding PNIPAM-stabilized CdS particles, where the molar ratio of PNIPAM–SH to CdS was 1/50 mol/mol. The resulting stable CdS solutions were purified via three-time centrifugation at 12 000 rpm for 1 h at 25 °C. Aqueous dispersions of stable PNIPAM-protected CdS QDs were prepared by directly redispersing the purified CdS QDs in deionized water. Note that such prepared CdS QD solution can be stable for more than 1 month at temperatures above LCST of PNIPAM. In contrast, a mixture of PNIPAM and the QD solution would precipitate at temperatures above the LCST. The fact indicates the covalent bonding of PNIPAM on QD surface. The dispersion concentrations used were 1×10^{-5} and 1×10^{-4} g/mL, respectively, in LLS and TEM measurements. To ensure complete dissolution, all the dispersions were kept at 4 °C for at least 24 h before the LLS measurement. All the dispersions were purified by a 0.45- μm Millipore (Hydrophilic Millex-LCR PTFE) filter.

Laser Light Scattering (LLS). A commercial spectrometer (ALV/DLS/SLS-5022) equipped with a multi- τ digital time correlator

(ALV5000) and a cylindrical 22 mW UNIPHASE He–Ne laser ($\lambda_0 = 632$ nm) as the light source was used. The incident beam was vertically polarized with respect to the scattering plane. The details of the LLS instrument and theory can be found elsewhere.²¹ In dynamic LLS, the Laplace inversion of each measured intensity–intensity time correlation function $G^{(2)}(q, t)$ in the self-beating mode can lead to a line-width distribution $G(\Gamma)$.^{22,23} For a pure diffusive relaxation, Γ is related to a translational diffusion coefficient D by $(\Gamma/q^2)_{c \rightarrow 0, q \rightarrow 0} \rightarrow D$ or further to a hydrodynamic radius R_h via the Stokes–Einstein equation, $R_h = (k_B T / 6\pi\eta_0) / D$, where k_B , T , and η_0 are the Boltzmann constant, the absolute temperature, and the solvent viscosity, respectively.

In static LLS, we can obtain the weight-average molar mass (M_w) and the z -average root-mean square radius of gyration ($\langle R_g^2 \rangle_z^{1/2}$, written as $\langle R_g \rangle$) of scattering objects in a dilute solution or dispersion from the angular dependence of the excess absolute scattering intensity, known as Rayleigh ratio $R_{vv}(q)$, on the basis of

$$\left(\frac{KC}{R_{vv}(q)} \right)_{c \rightarrow 0} \cong \frac{1}{M_w} \left(1 + \frac{1}{3} \langle R_g^2 \rangle_z q^2 \right) \quad \text{for } q \langle R_g^2 \rangle_z^{1/2} < 1 \quad (1)$$

where $K = 4\pi^2 n^2 (dn/dc)^2 / (N_A \lambda_0^4)$ and $q = (4\pi n / \lambda_0) \sin(\theta/2)$, with N_A , dn/dc , n , and λ_0 being Avogadro's number, the specific refractive index increment, the solvent refractive index, and the wavelength of the light in vacuum, respectively. However, for large particles, the following Guinier plot instead of the Zimm plot has to be used:

$$\left(\frac{KC}{R_{vv}(q)} \right)_{c \rightarrow 0} \cong \frac{1}{M_w} \exp\left(\frac{1}{3} \langle R_g^2 \rangle_z q^2 \right) \quad \text{for } q \langle R_g^2 \rangle_z^{1/2} > 1 \quad (2)$$

In one typical heating–cooling cycle, each aqueous solution of PNIPAM-stabilized QDs was heated or cooled inside the LLS spectrometer with a step of 1–2 °C. The precision of temperature control is ± 0.05 °C. At each temperature, the dispersion stood for 2–3 h so that the equilibrium could be reached. After it, both the DLS and SLS measurements were performed. The dn/dc value of 0.167 mL/g was used to estimate the weight-average molar mass (M_w) of the QDs.

Transmission Electron Microscopy (TEM). The morphologies of the aggregates during the cooling process were studied by TEM (Hitachi 800) with a 200 kV acceleration voltage. The samples for the TEM measurements were prepared by the deposition of one drop of dilute aqueous dispersion of PNIPAM(31K)-stabilized CdS QDs ($C = 1 \times 10^{-4}$ g/mL) on a copper grid coated with thin films of carbon at a desired temperature, and the solvent was removed by isothermal evaporation.

Fourier Transform Infrared Spectroscopy (FTIR). FTIR spectra were measured on a Nicolet Magna 750 IR spectrometer with a resolution of 4 cm^{-1} . In a typical experiment, 10 μL of PNIPAM solution in D_2O (0.020 g/mL) was added to a cell between two KRS-5 crystals with a space of 20 μm . The FTIR cell was attached to a metal holder and heated by a heat tape. An electronic thermometer with a precision of ± 0.1 °C continuously monitored the temperature of the cell holder.

Results and Discussion

Figures 1–3 summarize the temperature dependence of the average hydrodynamic radius ($\langle R_h \rangle$), the z -average root-mean-square radius of gyration ($\langle R_g \rangle$), and the average aggregation number ($\langle N_{\text{agg}} \rangle$) in aqueous dispersions of PNIPAM(31K)–CdS and PNIPAM(15K)–CdS QDs during one heating–cooling cycle, respectively. N_{agg} is calculated from the ratio of the apparent weight-average molar masses of the aggregates and individual PNIPAM-stabilized CdS QDs. They behave in a similar way.

(15) Otake, K.; Inomata, H.; Konno, M.; Saito, S. *Macromolecules* **1990**, *23*, 283.

(16) Kubota, K.; Fujishige, S.; Ando, I. *J. Phys. Chem.* **1990**, *94*, 5154.

(17) Wu, C.; Zhou, S. Q. *Phys. Rev. Lett.* **1996**, *77*, 3053.

(18) Wu, C.; Wang, X. H. *Phys. Rev. Lett.* **1998**, *79*, 4092.

(19) Siu, M.; Liu, H. Y.; Zhu, X. X. *Macromolecules* **2003**, *36*, 2103.

(20) Wuelfing, W. K.; Cross, S. M.; Miles, D. T.; Murray, R. W. *J. Am. Chem. Soc.* **1998**, *120*, 12696.

(21) Teraoka, I. *Polymer Solution*; John Wiley & Sons: New York, 2002

(22) Chu, B. *Laser Light Scattering*, 2nd ed.; Academic Press: New York, 1991

(23) Berne, B. J.; Pecora, R. *Dynamic Light Scattering*, Plenum Press: New York, 1976.

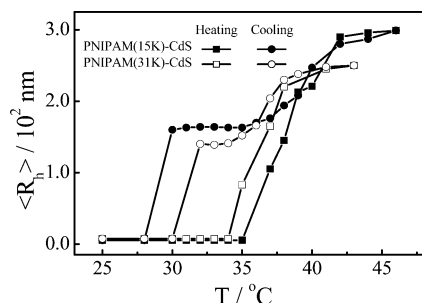


Figure 1. Temperature dependence of the average hydrodynamic radius ($\langle R_h \rangle$) of PNIPAM(31K)-CdS and PNIPAM(15K)-CdS QDs in water during one heating-and-cooling cycle. Each data point was obtained after the temperature equilibrium was reached.

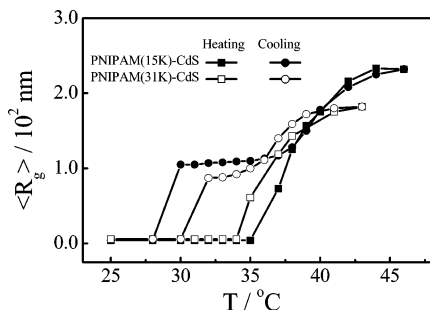


Figure 2. Temperature dependence of average radius of gyration ($\langle R_g \rangle$) of PNIPAM(31K)-CdS and PNIPAM(15K)-CdS QDs in water during one heating-and-cooling cycle. Each data point was obtained after the temperature equilibrium was reached.

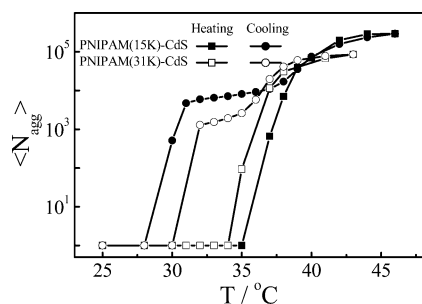


Figure 3. Temperature dependence of average aggregation number ($\langle N_{agg} \rangle$) of PNIPAM(31K)-CdS and PNIPAM(15K)-CdS QDs in water during one heating-and-cooling cycle. ($\langle N_{agg} \rangle$ is defined as $M_w(T)/M_w(25^\circ\text{C})$, where $M_w(T)$ and $M_w(25^\circ\text{C})$ the weight-average molar masses of the aggregates at temperature T and the single particle at 25°C , respectively. Each data point was obtained after equilibrium was reached.

Namely, in the heating process, the sharp increase of $\langle R_h \rangle$, $\langle R_g \rangle$, and $\langle N_{agg} \rangle$ at a certain temperature reveals the interparticle association. At higher temperatures, these values approach their respective constants, indicating the formation of stable QD aggregates. The CdS QDs with longer grafted PNIPAM chains undergo the association at lower temperature, which is reasonable because of the lower LCST of longer PNIPAM chains. The final average size of PNIPAM(15K)-CdS aggregate is larger than that of PNIPAM(31K)-CdS aggregate because shorter PNIPAM chains provide less stabilizing time than longer PNIPAM chains. This is why $\langle N_{agg} \rangle$ for PNIPAM(15K)-CdS QDs is much larger than that for PNIPAM(31K)-CdS QDs. In contrast, in the cooling process, $\langle R_h \rangle$, $\langle R_g \rangle$, and $\langle N_{agg} \rangle$ initially decrease with the decrease of dispersion temperature, and there is nearly no hysteresis observed. However, further decrease of dispersion temperature nearly results in no decrease of $\langle R_h \rangle$, $\langle R_g \rangle$, and $\langle N_{agg} \rangle$. The unexpected plateaus lead to a large hysteresis. Finally, the

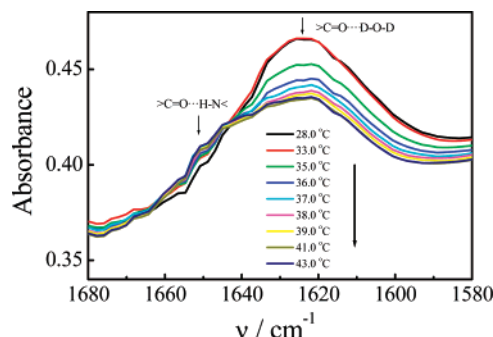


Figure 4. FTIR spectra of PNIPAM(31K)-CdS QDs in D_2O as a function of temperature, where the QDs concentration is 2.0×10^{-2} g/mL.

interparticle aggregates suddenly dissociate back into individual CdS QDs at a sufficiently low temperature.

In the study of the coil-to-globule and the globule-to-coil transitions of individual PNIPAM chains,¹⁸ a hysteresis was found and speculated to be due to the formation of some additional intrachain hydrogen bonds in the collapsed state.^{24,25} Later, Zhang et al.²⁶ observed a much clearer hysteresis in the heating-cooling cycle of PNIPAM chains grafted on a flat surface (polymer brushes). They attributed such a hysteresis to the persistence of some additional intra- and interchain hydrogen bonds formed because the temperature is not sufficiently low and the solvent is not sufficiently good to “melt” these additional hydrogen bonds. Further, Cheng et al.²⁷ used infrared spectroscopy to confirm that the hysteresis is indeed related to the formation of some additional hydrogen bonds in the collapsed state. The hysteresis was also studied by FTIR. Figure 4 shows the typical FTIR spectra of PNIPAM-CdS in the range $1680\text{--}1580\text{ cm}^{-1}$ at different temperatures. The band centered at 1625 cm^{-1} and the shoulder at 1650 cm^{-1} are ascribed to the hydrogen bonding ($>\text{C}=\text{O}\cdots\text{D}-\text{O}-\text{D}$ and $>\text{C}=\text{O}\cdots\text{H}-\text{N}<$).²⁴ As temperature increases, the weighting of the band at 1625 cm^{-1} decreases, indicating the dehydration of PNIPAM chains. On the other hand, the increase in the weighting of the shoulder at 1650 cm^{-1} with temperature indicates that hydrogen bonds between $>\text{N}-\text{H}$ and $\text{O}=\text{C}<$ groups in PNIPAM chains or the additional hydrogen bonds form. Note that the dehydration occurs at a temperature higher than LCST ($\sim 35^\circ\text{C}$). This is consistent with the LLS results above.

Therefore, we believe that the hysteresis in Figures 1–3 is also related to the additional hydrogen bonds formed at higher temperatures. It is these additional hydrogen bonds that hold individual QDs together, even though the dispersion temperature is lower than the LCST ($\sim 32^\circ\text{C}$) of PNIPAM.

Figures 1–3 show that the apparent association temperatures of PNIPAM(31K)-CdS and PNIPAM(15K)-CdS QDs in the heating process are 35 and 37°C , respectively, slightly higher than the LCST of linear PNIPAM chains free in a dilute solution. It has been reported before that the tethered polymer chains have a higher LCST or a lower UCST than their corresponding free chains.^{14,28} It has been attributed to the chain restriction on the surface, which makes the chain collapsing more difficult. On the other hand, relatively shorter PNIPAM chains ($31\ 000$ and $15\ 000$ g/mol) and a low concentration also push the LCST higher. The number of PNIPAM chains per CdS particles can be estimated

(24) Maeda, Y.; Higuchi, T.; Ikeda, I. *Langmuir* **2000**, *16*, 7503.

(25) Maeda, Y.; Nakamura, T.; Ikeda, I. *Macromolecules* **2001**, *34*, 1391.

(26) Liu, G. M.; Zhang, G. Z. *J. Phys. Chem. B* **2005**, *109*, 743–747.

(27) Cheng, H.; Shen, L.; Wu, C. *Macromolecules* **2006**, *39*, 2325.

(28) Zhang, W. A.; Zhou, X. C.; Li, H.; Fang, Y.; Zhang, G. Z. *Macromolecules* **2005**, *38*, 909.

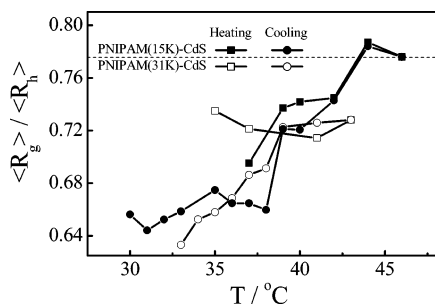


Figure 5. Temperature dependence of the ratio of average radius of gyration to average hydrodynamic radius ($\langle R_g \rangle / \langle R_h \rangle$) of resultant QD aggregates during one heating-and-cooling cycle.

from the ratio of the average molar mass of CdS particles and that of PNIPAM chains. On average, each CdS particle has two or three PNIPAM chains. Therefore, the grafting density has a slight effect on the association/dissociation of PNIPAM–CdS QDs.

Actually, in the cooling “plateau” region, $\langle R_h \rangle$, $\langle R_g \rangle$, and $\langle N_{\text{agg}} \rangle$ still slightly decrease, indicating gradual and slow dissociation of the QD aggregates as the temperature decreases. It is well-known that the ratio of $\langle R_g \rangle / \langle R_h \rangle$ can better reflect the structural or conformational change of a scattering object. This is because $\langle R_g \rangle$ reflects the density distribution of the chain in real physical space, while $\langle R_h \rangle$ is the radius of a hard sphere with the same translational diffusion coefficient under the same condition.²¹ For a random polymer chain in its good solvent, $\langle R_g \rangle / \langle R_h \rangle \sim 1.5$, while for a uniform hard sphere, $\langle R_g \rangle / \langle R_h \rangle \sim 0.774$.^{29,30} In the current case, at lower temperatures, individual PNIPAM-grafted CdS QDs have a core–shell structure. The core has a higher density than the polymeric shell, resulting in a ratio of $\langle R_g \rangle / \langle R_h \rangle$ lower than 0.774. However, $\langle R_g \rangle$ of individual QDs is too small to be measured. Therefore, we are unable to obtain initial values of $\langle R_g \rangle / \langle R_h \rangle$ of PNIPAM-stabilized CdS QDs before the association starts. The dash line in Figure 5 represents the ratio of $\langle R_g \rangle / \langle R_h \rangle$ for a uniform sphere. Figure 5 shows that, in the heating process, $\langle R_g \rangle / \langle R_h \rangle$ for PNIPAM(31K)–CdS QD aggregates slightly varies around 0.72, lower than 0.774 for a uniform hard sphere. For PNIPAM(15K)–CdS QDs, the aggregation leads to a slow increase of $\langle R_g \rangle / \langle R_h \rangle$ from ~ 0.70 to ~ 0.77 , indicating the formation of compact spherical aggregates at higher temperatures. Note that, in Figures 1 and 2, both $\langle R_h \rangle$ and $\langle R_g \rangle$ increase with the dispersion temperatures, but the increase of $\langle R_h \rangle$ is relatively slower than that of $\langle R_g \rangle$, presumably due to the shrinking of the PNIPAM shell.

To further confirm that the resultant QD aggregates have a spherical structure, we tried to fit the angular dependent scattering intensity with different structural factors $P(q)$.²¹ It has been well-known that,²¹ for a uniform hard sphere, a Gaussian sphere, and a Gaussian chain, their structure factors are $[3x^{-3}(\sin x - x \cos x)]^2$ ($x = q(5R_g^2/3)^{1/2}$), $[\exp(-1/3)x^2]$ ($x = qR_g$), and $[2x^{-2}(1 - x^{-2}(1 - \exp(-x^2)))]$ ($x = qR_g$), respectively. Figures 7 and 8 reveal a reasonable agreement between the experimental data and $P(q)$ of a Gaussian sphere for both PNIPAM(15K)–CdS and PNIPAM(31K)–CdS QD aggregates.

In the cooling process, $\langle R_g \rangle / \langle R_h \rangle$ decreases from $\sim 0.72 / \sim 0.77$ to ~ 0.64 for both the PNIPAM-stabilized CdS QDs. A combination of Figures 1, 2, and 5 reveals the swelling and dissociation of QD aggregates. The decrease of $\langle R_g \rangle / \langle R_h \rangle$ reflects that $\langle R_g \rangle$ decreases faster than $\langle R_h \rangle$ with the temperature. The

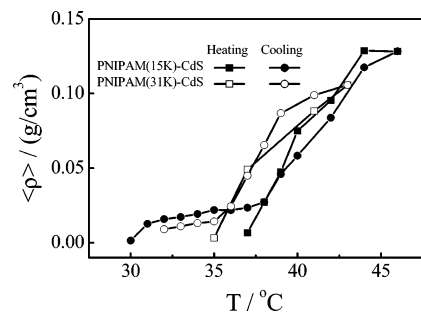


Figure 6. Temperature dependence of average chain density ($\langle \rho \rangle$) of resultant QD aggregates during one heating-and-cooling cycle, where $\langle \rho \rangle$ is defined as $M_{w,\text{agg}} / (4\pi \langle R_h \rangle^3 N_A / 3)$.

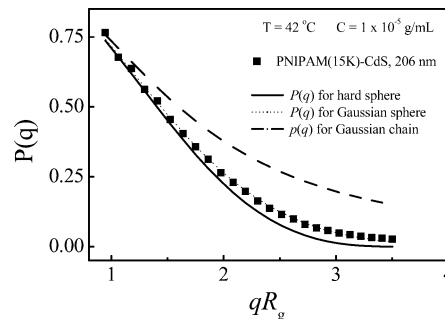


Figure 7. Comparison of measured structure factor with different calculated structure factors as a function of (qR_g) for PNIPAM-(15K)–CdS QD aggregates.

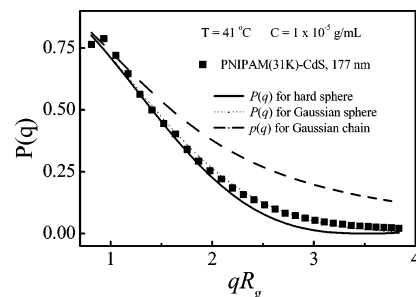


Figure 8. Comparison of measured structure factor with different calculated structure factors as a function of (qR_g) for PNIPAM-(31K)–CdS QD aggregates.

swelling of the PNIPAM shell increases $\langle R_h \rangle$ more and the dissociation of the aggregates results in the decrease of both $\langle R_g \rangle$ and $\langle R_h \rangle$. The swelling can be better reflected in the average chain density ($\langle \rho \rangle$) change, as shown in Figure 6, where $\langle \rho \rangle$ is defined as $M_w / (4\pi \langle R_h \rangle^3 N_A / 3)$ and M_w is the average molar mass of the aggregates.

As expected, the heating leads to the chain contraction, so $\langle \rho \rangle$ increases when the QDs starts to aggregate. At the initial stage, the density values of PNIPAM (15K)–CdS and PNIPAM (31K)–CdS particles at low temperature are 0.002 and 0.008 g/cm³, respectively. The low-density suggests that the aggregates contain a large amount of trapped water (>99%). In other words, PNIPAM chains are highly hydrated. Further increase of the temperature results in the collapse of the PNIPAM shell of each QD and the packing of QDs inside each aggregate so that $\langle \rho \rangle$ becomes higher. Also note that even at the fully collapsed state, the average chain density of PNIPAM/QDs composites is only slightly higher than 0.1, indicating that is difficult to form a bulk material from such formed QD aggregates ($\langle \rho \rangle \sim 1 \text{ g/cm}^3$). In the cooling process, $\langle \rho \rangle$ decreases with the temperature, indicating the chain swelling inside each aggregate. In the low-temperature range, the hysteresis is obvious. The complete dissociation of the aggregates only

(29) Burchard, W.; Schmidt, M.; Stockmayer, W. H. *Macromolecules* **1980**, *13*, 1265.

(30) Douglas, J. P.; Roovers, J.; Freed, K. F. *Macromolecules* **1990**, *23*, 418.

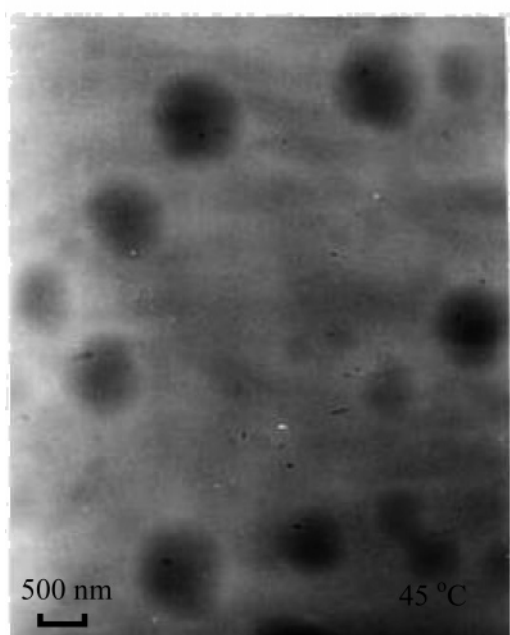
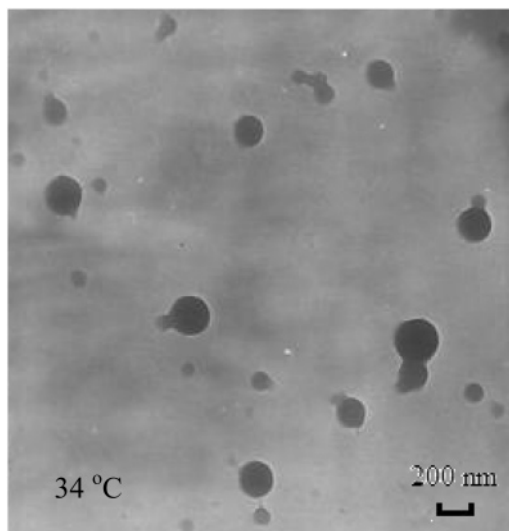


Figure 9. TEM images of PNIPAM(31K)-CdS QD aggregates at two different temperatures during the cooling process.

occurs at a temperature much lower than the aggregation temperature in the heating process, consistent with the previous observation of the temperature-induced conformational change of grafted PNIPAM chains on a flat surface.²⁶ The TEM measurements, as shown in Figure 9, at two different temperatures confirm the spherical structures of the PNIPAM-CdS QD aggregates during the cooling process. Note that the size and polydispersity of the aggregates determined by TEM are somewhat larger than those measured by laser light scattering. This is because of the aggregation of PNIPAM-CdS QDs on

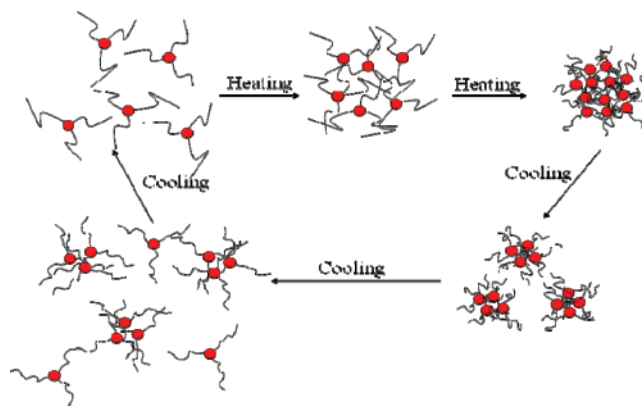


Figure 10. Schematic summary of association and dissociation of small PNIPAM-stabilized CdS QDs in water during one heating-and-cooling cycle.

the TEM grid induced by the dehydration of PNIPAM chains during the evaporation of water.

Conclusion

Water-soluble semiconductor CdS QDs can be effectively prepared and stabilized by grafting a layer of thermally sensitive linear PNIPAM chains on their periphery. The heating and cooling of the dispersion can induce the formation and fragmentation of spherical aggregates with small semiconductor QDs dispersed inside a PNIPAM matrix, as confirmed by LLS and TEM. In the heating process, the PNIPAM chains shrink and collapse at the LCST, leading to the interparticle aggregation. In the cooling process, the fragmentation and swelling of each QD aggregate lead to the opposite effect on the average size of the aggregates. Initially, the domination of fragmentation leads to a characteristic decrease of the average aggregate size in the cooling process. Further decrease of the temperature makes the swelling become dominating, so a plateau appears in the temperature dependence of the average aggregate size, resulting in an obvious hysteresis. Such a hysteresis in one heating-and-cooling cycle has been observed before for linear PNIPAM chains free in a dilute solution or a layer of grafted PNIPAM chains on a flat surface, which was first attributed to and later confirmed as some additional intra- and interchain hydrogen bonds between C=O and N-H groups. The association/dissociation is schematically summarized in Figure 10. These PNIPAM-stabilized CdS QDs are potentially useful as a “smart” and “tunable” material in biological applications.

Acknowledgment. The financial support of the Chinese Academy of Sciences (CAS) Special Grant (KJXC2-SW-H14), the National Natural Scientific Foundation of China (NNSFC) Projects (20534020 and 20574065), and the Hong Kong Special Administration Region (HKSAR) Earmarked Project (CUHK4037/06P, 2160298) is gratefully acknowledged.

LA703018P